THE EFFECTS OF COASTAL GEOMETRY ON TURBULENT MIXING IN UPWELLING FLOWS

Yu-Heng Tseng, Joel H. Ferziger
Environmental Fluid Mechanics Laboratory, Stanford University
Stanford, CA 94305-4020, USA
yhtseng@stanford.edu

Gwo-Hshiung Tzeng
Institute of Technology Management, College of Management, National Chiao Tung University
Hsin-Chu, Taiwan
ghtzeng@cc.nctu.edu.tw

ABSTRACT

Upwelling is responsible for a large fraction of the mixing in the ocean and is important to the biological productivity. We study this process by solving the Navier-Stokes (N-S) equations in generalized curvilinear coordinates using the numerical model of Zang and Street (1995). The influence of coastal perturbations such as capes on the large-scale structures and mixing is investigated. The structure of the instabilities is found to be of mixed baroclinic-barotropic type (Tadepalli and Ferziger, 2001). Nonlinear interactions moderate the growth of the large scales and generate 'fish-hook' structures. The Rayleigh-Taylor and mixed instabilities and fish-hook structures cause a sharp increase in the mixing. The mixing and stirring are quantified using a mixedness parameter and energy budgets (Tseng and Ferziger, 2001). Coastal perturbations modify the coherent structures which travel in the windward direction. The latter are not phase-locked by the cape. The cape produces strong vortex stretching due to the acceleration of the flow around it. The continued vortex stretching eventually results in vortex tearing in the cape vicinity. This process causes greater stirring than in the no-cape flow.

INTRODUCTION

Along coastlines, circulation is greatly influenced by coastal upwelling. In it, buoyancy, rotation, stratification, topography, and surface forcing are all significant. When the coastal wind is toward the equator and strong enough, the earth's rotation draws surface water away from the coastline. Strong and recurrent coastal upwelling occur off the west coasts of the United States mainly in spring and summer.

Several researchers have conducted laboratory experiments designed to study coastal upwelling flow. Narimousa and Maxworthy (1987,1985) created a two-layer stratified fluid in a rotating conical cylinder. The top disk was rotated differentially with respect to the system rotation to simulate a surface wind stress. As a result, the density interface elevated near the outer wall and, when the surface stress was strong enough, the interface intersected the surface and formed a front that continued to migrate offshore. The front was unstable under certain conditions and azimuthal waves appeared and grew to large amplitude. Zang and Street (1995) used large eddy simulations (LES) to study the upwelling flows. The domain resembles the laboratory experiment of Narimousa and Maxworthy. In our study, we extend this model to characterize the influence of the coastal perturbations on the properties of upwelling and enhancement of turbulent mixing.

NUMERICAL SIMULATION

Large eddy simulation is employed to simulate the upwelling experiments of Narimousa and Maxworthy (1987) with and without a cape, in which the wind stress is simulated by rotating the top lid relative to the tank at angular velocity $\Delta\Omega = 2\pi/\Delta T$, where ΔT is the rotation period of the lid.

Numerical formulation

Density varies only by about a few percent

in the ocean. Hence, we employ the Boussinesq approximation and the governing equations express mass, momentum and scalar conservation. At the top of the domain, the azimuthal velocity is $u_h = -\triangle\Omega \times r$. A no-slip condition is used for the tangential velocity while the normal velocity is zero on the top, side, and bottom walls. Periodic boundary conditions are used for the flow in the azimuthal (longshore) direction. The initial condition contains 'two-layer' stratified fluid and the density field is horizontally uniform.

The N-S equations are solved using a finite-volume technique. The equations for the resolved field are obtained by filtering the governing equations. The filtered equations are transformed into curvilinear coordinates while the Cartesian velocity components are retained. A non-staggered grid is used here. The method of fractional steps (a variant of the projection method), which splits the numerical operators and enforces continuity (Kim and moin, 1985) by solving a pressure Poisson equation, is employed here. All spatial derivatives are discretized using central differences with the exception of convective terms. These terms are discretized using QUICK in which the velocity components on the cell faces are computed from the nodal values using a quadratic interpolation scheme. The convective terms in the scalar transport equation are discretized using SHARP (Leonard, 1988), a monotonic approximation that has the ability to deal with convectively dominated flows. The momentum equations are solved using approximate factorization. Details of the method can be found in Zang (1993).

This flow contains a wide range of scales, making it prohibitively expensive to directly simulate all of the scales. The idea of LES is to simulate the large scale structures and modeling the small scales. The sub-filter scale (SFS) motions of many flows may be treated with a single model. We use dynamic subfilter scale model with local averaging for computing the influence of small scales in the upwelling flow. The model predicts the correct asymptotic behavior near the boundaries and allows energy backscatter (Germano et al., 1991). The details are given in Zang (1993).

Description of the simulations

We conducted two sets of simulations, one with and one without coastline perturbations. One quadrant of the tank is simulated using periodic boundary conditions in the azimuthal direction. The domain is an annular region with a sloping bottom (see Fig. 1 for a typical grid). The filtered Navier-Stokes equations are solved in the rotating frame. The initial vertical density distribution has a hyperbolic tangent profile approximating the two layer structure in the experiments. There is no initial azimuthal or horizontal density variation.

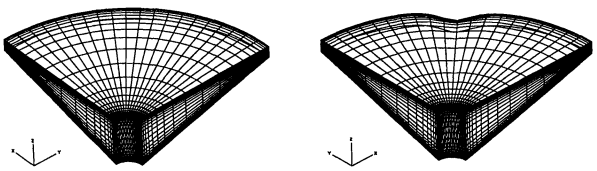

(a) (b)

Figure 1: (a) Grid for numerical simulation of upwelling flow. (b) The grid for numerical simulation with cape. (Every fourth grid is shown)

The geometry for the simulations with a cape is obtained from the function defined as 'Witch of Agnesi' which relates the radial excursion distance (d) to the azimuthal angle(Fig. 1(b)). $d(\theta)$ has a maximum at $\theta = 45°$. The cape geometry defined above is slightly different from the cylinder of radius R_c used in the laboratory experiments of Narimousa and Maxworthy (1987). However, the maximum width of the cape is chosen as the cape radius (R_c) in their experiments (case: cape M) which was designed to be representative of the coastline perturbations. Since we employ periodic boundary conditions in the azimuthal direction, these simulations are representative of an upwelling flow with four capes, one in each quadrant. The boundary conditions were described above.

The parameters of the simulation are given in Tables 1. The dominant instability mechanisms are inviscid. The Reynolds number ($Re = \rho U_p R_0/\mu$ where U_p the disk edge velocity, R_0 the outer radius of the annulus, ρ the density and μ the viscosity of water) of the simulations must be lower than that of the experiments for computational efficiency. This is permitted because the flow behavior becomes independent of Re when the latter is large enough. Other non-dimensional parameters include the Rossby number and the layer Froude numbers. The Rossby number is $Ro = U_p/f(R_0 - R_1)$. The layer Froude numbers are defined as $f^2\lambda_s^2/g'h_{10}$ where λ_s

Tank Rotation $\Omega(s^{-1})$	2.27
Lid Rotation $\Delta\Omega(s^{-1})$	0.185
Total Depth H (m)	0.20
Density Diff. $\Delta\rho(kg/m^3)$	18
Tank Radius $R_0(m)$	0.45
Slope	0.27
Reynolds number Re	2995
Schmidt number Sc	723

Table 1: Parameters of the simulations (Narimousa and Maxworthy, 1987)

is the theoretical stationary width of the density front, $g' = g\Delta\rho/\rho_1$ is the reduced gravity and h_{10} is the initial upper-layer depth. The spin-up time (Linden and Heijst, 1984), used here as the reference time scale, is $t_s = (h_{10}/\Delta\Omega)((\Omega+\Delta\Omega)/\nu)^{1/2}$ where $\Delta\Omega$ is the differential lid angular velocity and Ω is the tank rotation angular velocity.

EFFECTS OF COASTAL PERTURBATION ON LARGE SCALE

Narimousa and Maxworthy (1987) conducted a set of laboratory experiments on the effect of coastline perturbations. Their results show that maximum upwelling tends to occur on the downstream side of a cape. They suggested, however, that the strong upwelling observed near Cape was primarily caused by the local bottom topography and not the cape itself. Here, we focus on the modification of instabilities by a coastal perturbation and quantify the influence.

Fig. 2 compares the scalar field with and without the coastline perturbation. The primary front is drawn closer to the 'coastline' on the downstream side of the perturbation. The front downstream of the cape is wider than the no-cape front (Fig. 2). A large perturbation in the azimuthal velocity is observed just downstream of the cape as shown in Fig. 3 and coincides with the separation zone.

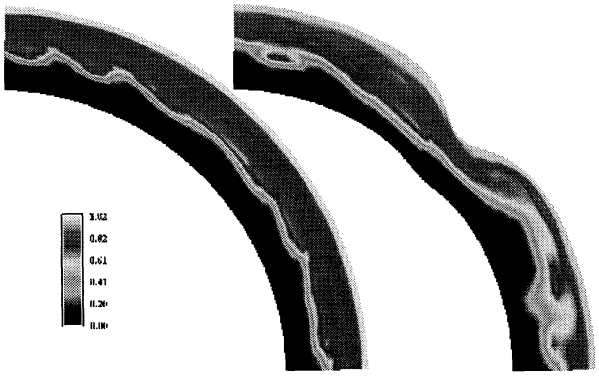

Figure 2: Density field in the neighborhood of the primary front with (right) and without (left) the coastline perturbation at $t = t_s$ and $z = 0.94h$.

Narimousa and Maxworthy (1987) indicated

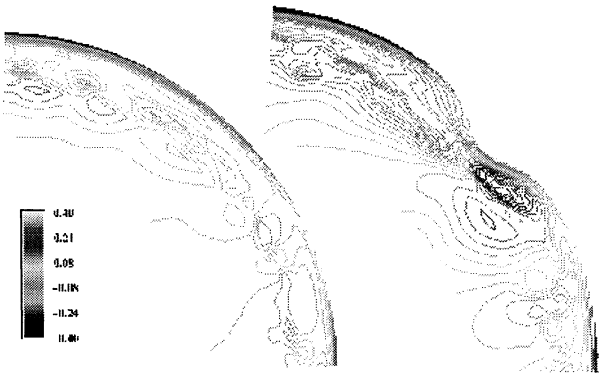

Figure 3: Azimuthal velocity perturbation in the neighborhood of the primary front with (right) and without (left) the coastline perturbation at $t = t_s$ and $z = 0.94h$.

that baroclinic waves interact with standing waves on the downstream side of the cape. Their observations were based on visual examination of the features observed in the experiments; no quantitative measurements were made to confirm the existence of the standing waves. Our simulations (similar to case:M in their experiments) suggest that the waves on the surface front are the result of mixed baroclinic-barotropic instability and move in the direction of the surface forcing (clockwise) in the rotating frame (Fig. 4). These waves are modified by the cape, mainly in the troughs (which are close to the 'coastline'). The front excursions are more irregular (Fig. 4) than without the cape. In the latter case, they are nearly periodic (Fig. 2).

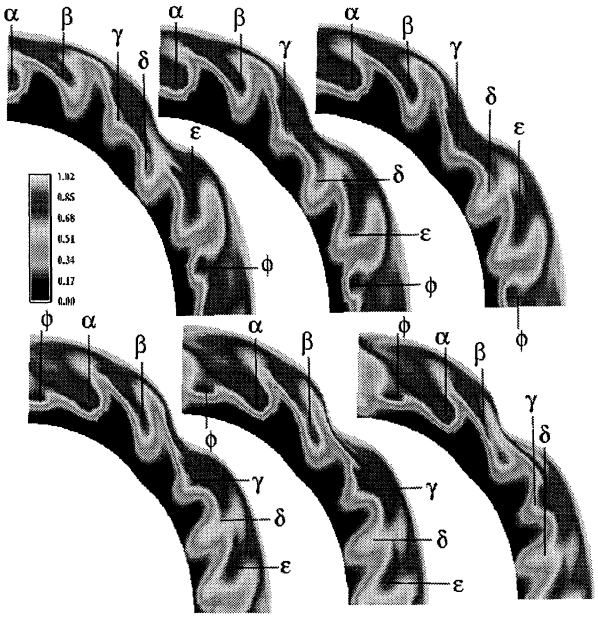

Figure 4: Density field in the neighborhood of the primary front at $t = 1.64t_s$(top left), $t = 1.66t_s$(top middle), $t = 1.68t_s$(top right), $t = 1.71t_s$(bottom left), $t = 1.74t_s$(bottom middle), $t = 1.76t_s$(bottom right) and $z = 0.9h$.

The front excursions are caused by the pres-

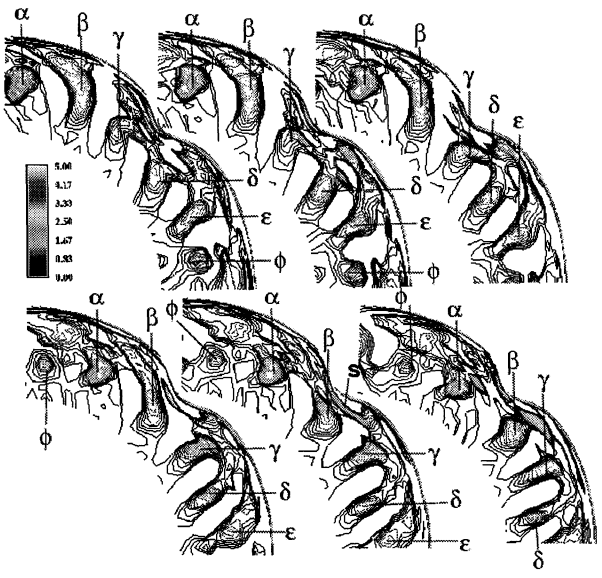

Figure 5: Absolute vertical vorticity in the neighborhood of the primary front at $t = 1.64t_s$(top left), $t = 1.66t_s$(top middle), $t = 1.68t_s$(top right), $t = 1.71t_s$(bottom left), $t = 1.74t_s$(bottom middle), $t = 1.76t_s$(bottom right) and $z = 0.9h$.

ence of large-scale vortices (marked $\alpha - \phi$ in Fig. 4). The vortices are elongated by the influence of the cape (Fig. 5). As vortex β moves clockwise, it is stretched by the strain created by the acceleration of the fluid passing over the cape. Fig. 5 shows the absolute vertical vorticity at the same times as in Fig. 4. As the flow evolves, the surface front (Fig. 4) meanderings increase, causing distortion of the density front. All the vortices are elongated as they have already moved past a cape. (Recall that the periodicity implies that there are four capes.) As we shall see later, increased stretching of the front results in increased mixing. The dynamics can be best described in terms of the motion of a vortex; we focus on the one labeled β. Continued stretching results in tearing of the vortex (Fig. 5, lower-middle panel).

EFFECTS OF COASTAL PERTURBATION ON TURBULENT MIXING

As noted above, it is widely believed that coastline perturbations and topography have a significant effect on coastal currents, fronts, and upwelling and are responsible for the major features observed in satellite infrared (IR) images and enhanced mixing. It is very difficult to quantify mixing in either field measurements or laboratory experiments because very detailed data are required. In this study, we quantify mixing by using a mixedness parameter (M) as a global measure of mixing and by computing the reference potential energy (RPE).

Mixing parameter

The mixedness parameter defined below measures the fraction of the fluid that has been mixed. This mixedness parameter M is essentially the one proposed by Roshko (1976) for the mixing of different velocities and is defined by:

$$M(t) = \frac{1}{V}\int_V c(1-c)dV = \overline{c} - \overline{c^2} \qquad (1)$$

where V is the total volume of the domain, $\overline{c} = \frac{1}{V}\int_V c dV$, $\overline{c^2} = \frac{1}{V}\int_V c^2 dV$ and $c = (\rho - \rho_0)/\Delta\rho$, ρ_m is the density of the fluid in the upper layer (the minimum density found in the flow), and $\Delta\rho = \rho_M - \rho_m$ is the density difference between the lower and upper layers. Since $0 \leq c \leq 1$, $M = 0$ and $M = 0.25$ for the completely unmixed and fully mixed situations, respectively. Fig. 6 shows the evolution of the mixedness parameter in the upwelling flow with and without the cape. The observed mixedness is much smaller than 0.25, since mixing occurs only in a small portion of the flow. The amount of the mixed fluid increases monotonically with time as it must. Greater mixing is observed in the case of cape flow due to the larger front excursions and vortex stretching described above. The sharp increase of mixing in event E_1 is due to the initial Rayleigh-Taylor instability. Event E_2 is due to the onset of the mixed-instability of the front and the event E_3 is due to the formation of the fish-hook structures. The definition of the mixedness parameter is appropriate since its rate of change is positive definite and is proportional to the scalar dissipation χ:

$$dM/dt = k\int \nabla c \cdot \nabla c \, dV = \propto \chi \qquad (2)$$

which again indicates why M is a monotonic function of time.

Energy budgets

The reference potential energy is a direct measure of potential energy change due to irreversible diapycnal mixing (Tseng and Ferziger, 2001; Winters et al., 1995). Energy budgets thus provide another index for quantifying mixing. We use the RPE to evaluate irreversible mixing. The reference potential energy state has the minimum potential energy that can be obtained through adiabatic

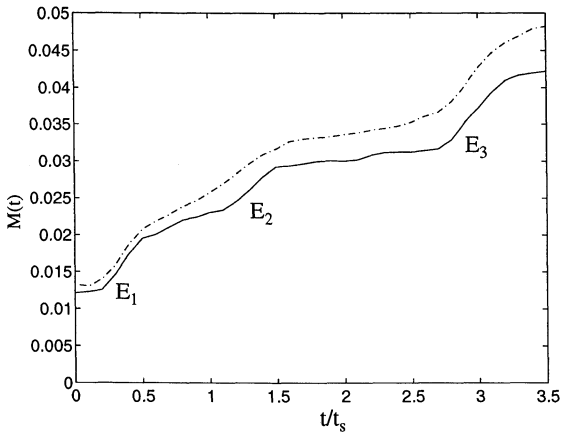

Figure 6: Mixedness parameter for upwelling flow with (−·) and without coastline (−) perturbation.

redistribution of the density (Winters et al., 1995). Tseng and Ferziger (2001) developed an efficient approach for calculating the RPE through the probability density function (pdf). The approach requires significantly less computation than the standard approach, especially in three dimensions. We apply the pdf approach to the investigation of mixing in upwelling flow. The RPE is defined as

$$RPE = \int_{\rho_m}^{\rho_M} \rho g Z_r(\rho) d\rho \qquad (3)$$

where ρ_m and ρ_M are minimum and maximum values of the density. Z_r is the reference state of density ρ. For an arbitrary domain with complex geometry, Z_r can be obtained from

$$\int_0^{Z_r(\rho)} A(z)dz = V \int_\rho^{\rho_M} P(\tilde{\rho})d\tilde{\rho} \qquad (4)$$

where $A(z)$ is the horizontal sectional area. $P(\tilde{\rho})$ is the probability density function of the domain V and is defined in terms of the volume integral of a delta function

$$P(\tilde{\rho}) \equiv \frac{1}{V}\int_V \delta(\tilde{\rho} - \rho)dV \qquad (5)$$

Note that the reference state profile $Z_r(\rho)$ is a monotonic function of the density ρ and is dimensionally a length. Only molecular mixing can alter the pdf of density field thus change the reference potential energy. The evolution of the energy budgets in the cases with and without the cape is shown in Fig. 7. Both RPE and TPE are slightly greater in the simulation with coastal perturbation. This increase is due to the mixing being very localized and results in greater available potential energy (APE) which is the difference between TPE and RPE. The evolution of the RPE and TPE in the two cases are quite similar. Fig 8 shows the corresponding instantaneous rate of RPE and TPE. Roughly three peaks appear, corresponding to the three mixing events described in previous section. Note that the peak of the TPE growth rate at event E_3 is less than that at events E_1 and E_2 because the fish-hook generation process is more localized than the others. The increased irreversible mixing at the later stages of evolution mainly results from the increases interface area between the bodies of fluid.

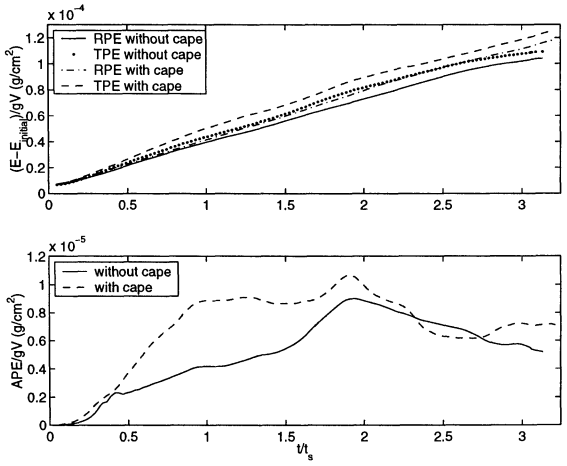

Figure 7: (a) The evolution of RPE and TPE. The initial RPE has been subtracted. (b) The evolution of APE.

APE is the portion of potential energy available for conversion to kinetic energy. The TPE in the cape case generates significant potential energy difference and thus greater global stirring as the instability develops (Fig. 7). This is as expected. The APE is primarily located at the upwelling front and increases as the front migrates. Fig. 9 shows the instantaneous rate of the increase of the APE. The transfer between kinetic energy and available potential energy is significant when the instability occurs, implying that most of the energy involved in the upwelling process is stored as APE. Slightly greater stirring occurs in the simulation with the cape.

CONCLUSION

The aim of this study is to further understand the effects of coastal perturbation on the features of coastal upwelling and the enhancement of mixing using LES. The cape produces strong vortex stretching due to the acceleration of the flow around it. The continued vortex stretching eventually results in vortex tearing in the cape vicinity. Greater mixing and stirring rates are found as the instabilities occur and shows more available potential energy in mixed-type instability and fish-hook structure.

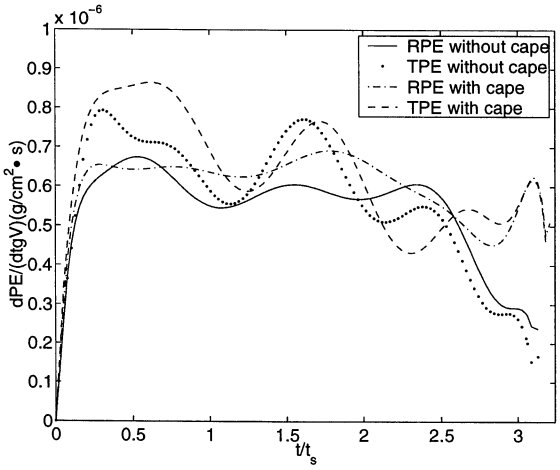

Figure 8: The instantaneous rate of RPE and TPE (with (–·) and without coastline (-) perturbation).

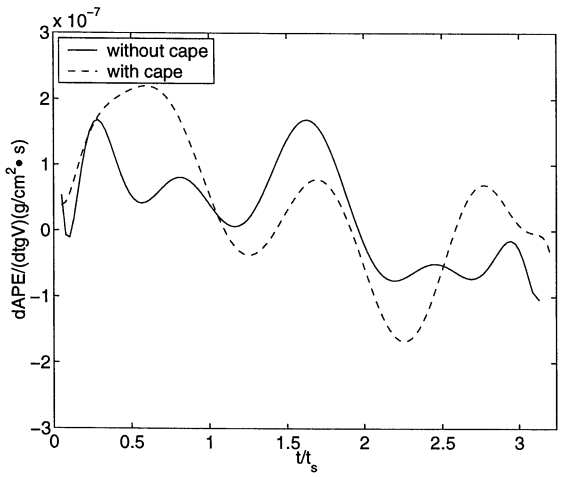

Figure 9: The instantaneous rate of APE without (-) and with coastline (–) perturbation).

A small cape in the simulation increases the RPE and APE, which implies more stirring locally thus enhancing irreversible mixing near the coastal boundary. This is not surprising and results from the global property of the APE. More details of the local effects of geometry and bathymetry will be investigated next.

REFERENCE

Germano, M., Piomelli, U., Moin, P. and Cabot, W. H., 1991, "A dynamic sub-grid scale eddy viscosity model",*Phys. Fluids*, A(3), pp. 1760-1765.

Kim, J. and Moin, P., 1985, "Application of a fractional-step method to incompressible Navier-Stokes equations", *Journal of Comput. Phys.*, Vol. 59, pp.308-323.

Leonard, B. P., 1988, "Third-order multidimensional Euler/Navier-Stokes solver", *AIAA/ASME/SIAM/APS first National Fluid Dynamics Congress*, pp.226-231.

Linden, P. F. and Van Heijst, J. F., 1984, "Two-layer spin-up and frontogenesis", *J. Fluid Mech.*, Vol. 143, pp. 69-94.

Narimousa, S. and Maxworthy, T., 1987 "On the effects of coastline perturbations on coastal currents and fronts", *J. Phys. Oceanogr.*, Vol. 17, pp. 1296-1303.

Narimousa, S. and Maxworthy, T., 1985, "Two-layer model of shear-driven coastal upwelling in the presence of bottom topography", *J. Fluid Mech.*, Vol. 159, pp. 503-531.

Roshko, A., 1976, "Structure of turbulent shear flows: A new look", *AIAA Journal*, Vol. 14, pp.1349-1357.

Tadepalli, S. and Ferziger, J. H., 2001 "Simulation of coastal upwelling. I. Linear stability and the early turbulent regime", *Submitted to J. Phy. Oceanogr.*.

Tseng, Y. H. and Ferziger, J. H., 2001 "Mixing and available potential energy in stratified flows", *Phys. Fluids (in press)*.

Winters, K. B., Lombard, P. N., Riley, J. J. and D'Asaro, E. A., 1995, "Available potential energy and mixing in density-stratified fluids", *J. Fluid Mech.*, Vol. 289, pp.115-128.

Zang, Y., 1993, *On the development of tools for the simulation of geophysical flows*, PhD thesis, Stanford University.

Zang, Y. and Street, R. L., 1995, "Numerical simulation of coastal upwelling and interfacial instability of a rotating and stratified fluid", *J. Fluid Mech.*, Vol. 305, pp. 47-75.